Extended Abstracts of the 2010 International Conference on Solid State Devices and Materials, Tokyo, 2010, pp1134-1135

Electrical detection of Spin Transport in Si using High-quality Schottky Contacts

K. Hamaya[1,2], Y. Ando[1,3] and M. Miyao[1]

[1]Department of Electronics, Kyushu University, 744 Nishi-ku, Fukuoka 819-0395, Japan
Phone: +81-92-802-3738, E-mail: hamaya@ed.kyushu-u.ac.jp
[2]PRESTO-JST, 4-1-8 Honmachi, Kawaguchi, Saitama 331-0012, Japan
[3] INAMORI FRC, Kyushu University, 744 Nishi-ku, Fukuoka 819-0395, Japan ,

1. Introduction

Because of the ultimate scaling limits of the complementary metal-oxide-semiconductor (CMOS) transistors, spin-based electronic (spintronic) technologies have been watched. In particular, group-IV semiconductor spintronics, compatible with existing Si-based semiconductor technologies, is now being required.

In addition, since Si has been predicted to be a semiconductor with enhanced spin lifetime and spin-transport length due to low spin-orbit scattering and lattice inversion symmetry, spin transport across 10 ~ 350 μm-Si channels can be detected in Si-based spin devices.[1].

In this paper, we first demonstrate high-quality epitaxial growth of ferromagnetic Fe_3Si, which is a Heusler compound, on Si by means of low-temperature molecular beam epitaxy (LTMBE) [2]. Second, we explain the Fe_3Si/n^+-Si/n -Si tunnel contacts to realize highly efficient spin injection and detection across the Schottky tunnel barrier. Finally, we demonstrate electrical spin injection and detection in a Si channel using such a high-quality spin injector and detector. [3]

2. Experimental details

25 nm-thick Heusler-type Fe_3Si films were grown on n-Si(111) (~10^{15} cm^{-3}) by LTMBE at 130 ~ 200°C [2]. During the growth, two-dimensional epitaxial growth was confirmed by the observation of reflection high energy electron diffraction (RHEED) patterns. Their crystal structures were characterized by means of cross-sectional transmission electron microscopy (TEM) and nano-beam electron diffraction (ED).

Also, to demonstrate electrical spin injection and detection in Si, we firstly inserted a heavily doped n^+-Si layer (~10^{20} cm^{-3}) between Fe_3Si and n-Si (~10^{15} cm^{-3}) [3]. Next, we fabricated lateral four-probe devices with one Co/Fe_3Si injector and one Fe_3Si detector for nonlocal spin-valve measurements [4-9]. The nonlocal voltage (NLV) measurements were performed by a dc method for the current-voltage scheme shown in Fig. 2(a), where external magnetic fields (B) were applied parallel to the long axis of the contacts in the film plane.

3. Results and Discussion

Figure 1(a) shows a representative cross-sectional transmission electron microscopy (TEM) image of an Fe_3Si/Si(111) structure grown by LTMBE. Almost no marked roughness and no reaction layer are identified at the interface between Fe_3Si and Si. Nanobeam electron diffraction patterns of the Fe_3Si layers are also presented in the inset of Fig. 1(a). We can see evident superlattice diffractions, (111) and (113), caused by the presence of the DO_3-ordered structures (white broken circles). These structural characterizations reveal that the high-quality formation of the ordered single-crystal Fe_3Si layers has been realized even on Si [2].

Next, we grew the Fe_3Si/n^+-Si/n -Si Schottky-tunnel contacts, as described in the experimental section. To evaluate electrical properties of the contacts, we fabricated two different Schottky diodes (~ 1 mm in diameter) with and without the n^+-Si layer. Here, we define these Schottky diodes as Diode A (with the n^+-Si layer) and Diode B

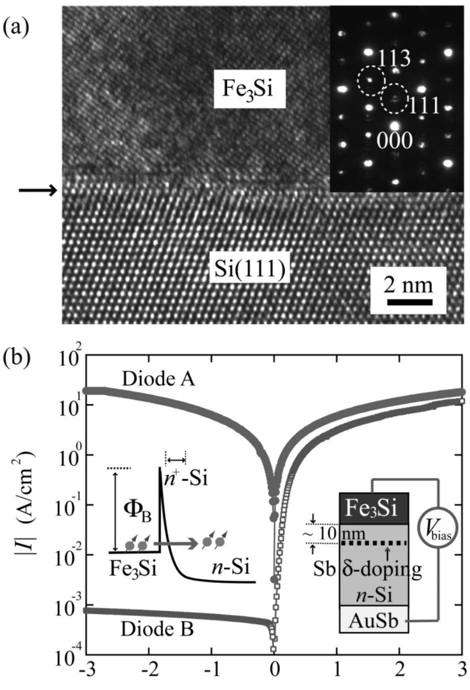

Fig.1. (a) A cross-sectional high-resolution TEM image of a representative Fe_3Si/Si(111) interface [2]. The inset shows nanobeam electron diffraction patterns of the epitaxial Fe_3Si layer. The zone axis is parallel to the[1-10] direction. (b) I-V characteristics of the fabricated Fe_3Si/Si Schottky diodes at 300 K [3]. The right and left insets show schematic illustrations of the Fe_3Si/Si(111) Schottky diode structure and an energy diagram of the conduction band for Fe_3Si/Si(111) with an n^+-Si layer in $V_{bias} < 0$, respectively.

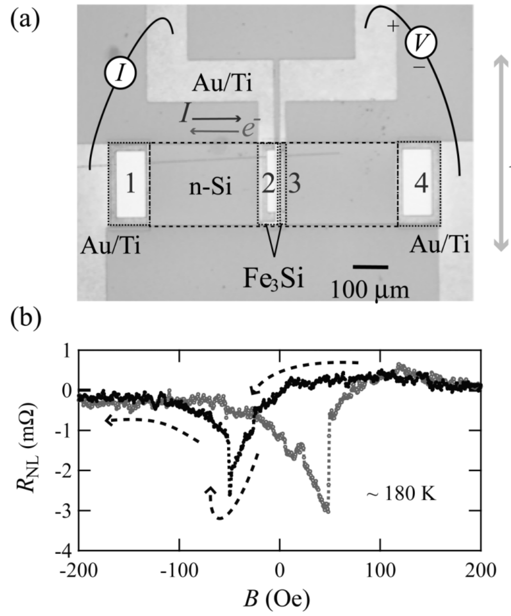

Fig.2. (a) An optical micrograph of the lateral four-probe device structure with Fe_3Si/n^+-Si/n-Si Schottky-tunnel contacts. (b) Non-local resistance, ($R_{NL} = \Delta V_{NL}/|I|$), versus external magnetic field B, measured at 180 K at I = 5 mA.

(without the n^+-Si layer). A schematic illustration of Diode A is shown in the inset of Fig. 1(b). The main panel of Fig. 1(b) presents absolute values of the current density, $|I|$, as a function of bias voltage (V_{bias}) for both Diode A and B. These characteristics were reproduced for ten devices. Typical rectifying behavior of a conventional Schottky diode is seen for Diode B, while we find almost symmetric behavior with respect to V_{bias} polarity for Diode A. Note that the reverse-bias $|I|$ ($|I_{rev.}|$) for Diode A is extremely large more than four orders of magnitude compared to that for Diode B. From the temperature-dependent $|I_{rev.}|$ (not shown here), it was indicated that Diode B shows the thermionic emission electron transport over a Schottky barrier (Φ_B = 0.61 eV). Using such contacts (without the n^+-Si layer), we could not detect spin-polarized carriers electrically due to additional resistance originating from a wide width of the depletion region (~500 nm). In contrast, we identified that $|I_{rev.}|$ for Diode A shows almost no variation with decreasing temperature, indicating that thermionic emission does not dominate. Namely, we can expect to achieve spin injection in Si across a Schottky tunnel barrier consisting of the epitaxially grown Fe_3Si/Si interface, as schematically shown in the left inset of Fig. 1(b).

We also fabricated four-probe lateral spin devices with the Fe_3Si/Si Schottky-tunnel-barrier contacts, as shown in Fig. 2(a), where the lateral geometries have been utilized by lots of researchers for the detection of spin transport in nonmagnetic channels [4-9]. The fabrication processes were shown in our previous article [3]. By using one Co/Fe_3Si injector and one Fe_3Si detector, we can distinguish between magnetization reversal processes of the spin injector and detector under NLV measurements. Figure 2(b) shows a representative NL resistance, $(V-V_0)/|I|$, as a function of B at 180 K, where V, V_0, and I are NLV, the subtracted background voltage [6-9], and the applied current (I = 5 mA), respectively. Clear hysteretic behavior is seen at ~180 K. This feature was strongly related to the relative magnetization orientation between the spin injector and detector. We also demonstrated clear sign changes in NLV by switching the polarity of the injected current. These are consistent with those of the silicon- and graphene-NL spin-valve devices [7,8]. Thus, these features are evident demonstrations of the electrical spin injection and detection in Si using Fe_3Si/Si Schottky-tunnel-barrier contacts. These results will open a road for Si-based spintronic devices.

4. Conclusions

We have demonstrated high-quality epitaxial growth of ferromagnetic Fe_3Si films which can be used as a spin injector and detector for Si channels. And then, we realized Schottky-tunnel contacts by an insertion of an n^+-Si layer between Fe_3Si and n-Si. Using the Schottky-tunnel contacts, we clearly detected nonlocal spin-valve hysteresis loops in lateral four-probe devices at ~ 180 K.

Acknowledgements

K.H. and M.M. acknowledge Prof. H. Itoh, Prof. T. Kimura, Dr. K. Sawano for theoretical and experimental supports. This work was partly supported by a Grant-in-Aid for Scientific Research on Priority Area from the MEXT, PRESTO from JST in Japan.

References

[1] I. Appelbaum et al., Nature **447** (2007) 295; Phys. Rev. Lett. **99** (2007) 177209; Phys. Rev. Lett. **103** (2009) 117202.
[2] K. Hamaya *et al.*, Appl. Phys. Lett. **93** (2008) 132117.
[3] Y. Ando *et al.*, Appl. Phys. Lett. **94** (2009) 182105.
[4] F. J. Jedema *et al.*, Nature **416** (2002) 713.
[5]T. Kimura and Y. Otani, J. Phys. Cond.Mat. **19** (2007) 165216.
[6] X. Lou *et al.*, Nat. Phys. **3** (2007) 197.
[7] O. M. J. van 't Erve *et al.*, IEEE Trans. Electron Devices **56** (2009) 2343.
[8] M. Shiraishi *et al.*, Adv. Funct. Mater. **19** (2009) 3711.
[9] T. Sasaki *et al.*, Appl. Phys. Lett. **96** (2010) 122101.